

Effect of CT Specimen Thickness on the Mechanical Characteristics at the Crack Tip of Stress Corrosion Cracking in Ni-based Alloys

Cui Yinghao¹, Xue He¹ and Zhao Lingyan²

¹ School of Mechanical Engineering, Xi'an University of Science and Technology, Xi'an 710054, China

² School of Science, Xi'an University of Science and Technology, Xi'an 710054, China

xue_he@hotmail.com

Abstract. It's important to obtain accurate stress corrosion crack(SCC) growth rate for quantitative life prediction of components in nuclear power plants. However, the engineering practice shows that the crack tip constraint effect has a great influence on the mechanical properties and crack growth rate of SCC at crack tip. To study the influence of the specimen thickness on the crack tip mechanical properties of SCC, the stress, strain and C integral at creep crack tip are analyzed under different specimens thickness. Results show that the cracked specimen is less likely to crack due to effect of crack tip constraint. When the thickness ratio B/W is larger than 0.1, the crack tip constraint is almost ineffective. Value of C integral is the largest when B/W is 0.25. Then specimen thickness has little effect on the value of C integral. The effect of specimen thickness on the value of C integral is less significant at higher thickness ratio.

1. Introduction

Ni-based alloy 600 is widely used in nuclear primary pressure vessel and dissimilar metal welded joints due to its good high temperature corrosion resistance and mechanical properties. The stress corrosion cracking (SCC) caused by crack tip creep in high temperature water environment is one of the important factors lead to the failure of structures [1]. Therefore, it is very important to obtain accurate creep crack propagation rate for quantitative prediction nuclear structure life [2-3]. Influence of the specimen thickness constraint on creep crack tip mechanical field is considered to correlate the creep rupture mechanics parameters with the structural crack propagation rate, and evaluate the structural integrity and the life prediction. Practice shows that the crack tip constraint has a great influence on the mechanical properties at the creep crack tip.

The crack tip constraint is usually controlled by the specimen geometry, the crack size, and the loading mode [4]. The influence of materials and structures fracture behavior [5] and crack tip constraint, quantitative characterization of constraint parameters [6-8], and the law of influence and mechanism of compound restraint on CGR [9] were studied by many scholars.

Different thickness finite element model is established by compact tension specimen using Ni-based Alloy 600. The micro-mechanical properties of crack tip region and the main parameters of SCC crack propagation rate are studied. The influence of CT specimen thickness on the fracture parameters



at creep crack tip of Ni-based Alloy is further analyzed, which is of great significance for the study of SCC crack initiation and propagation behavior.

2. Finite element modeling

2.1. Specimen model

Compact tensile specimen with prefabricated crack is used as the research object. 1T-CT specimen geometry is shown in Figure 1, which is coincidence with the American Society for Experimental and Materials Standards ASTM E399-90 standard [10]. The specimen width $W=50$ mm, the crack length $a = 0.5W$, the sample thickness is B , and the value of B/W is 0.05, 0.1, 0.2, 0.3 and 0.4, respectively.

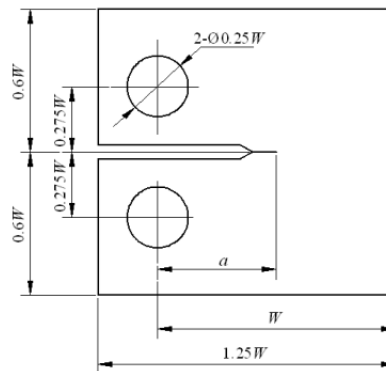


Figure 1. Geometry size of 1T-CT specimen

The finite element mesh of the 1T-CT global model and the local region of the crack tip are shown in Figure 2 when the $B/W = 0.05$, 8-node linear brick (C3D8) is used in simulation and total number is 138 820. To obtain a more accurate crack tip stress-strain, the mesh is refined at the crack tip and the total number at cracked local area is 42 680.

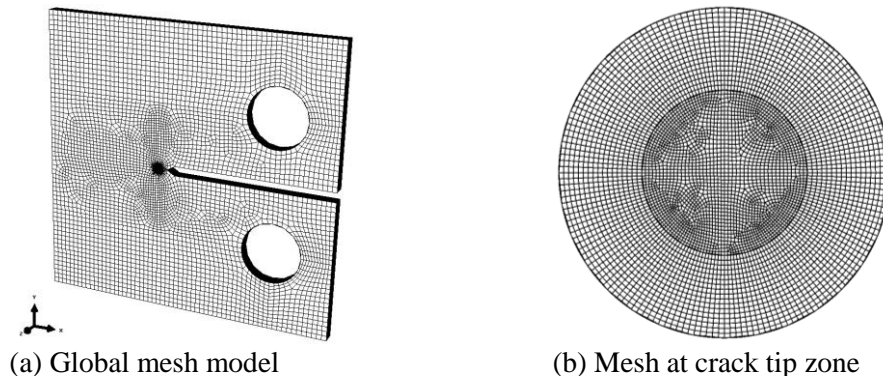


Figure 2. Finite element mesh model of 1T-CT

2.2. Material model

The Ni-based Alloy 600 is a power-hardened material whose constitutive relationship is usually characterized by the Ramberg-Osgood relationship [11], and its form is as follows:

$$\frac{\varepsilon}{\varepsilon_0} = \frac{\sigma}{\sigma_0} + \alpha \left(\frac{\sigma}{\sigma_0} \right)^n \quad (1)$$

Where ε is the strain, including elastic and plastic strain. σ is the total stress; ε_0 is the yield strain of the material, σ_0 is the yield stress of the material, and n is the strain hardening exponent of the material, α is the offset coefficient of the material.

The creep rate is calculated using the power law model [12-13] in the FEM calculation:

$$\dot{\epsilon}_{cr} = A\sigma^n t^m \quad (2)$$

Where $\dot{\epsilon}_{cr}$ is the creep strain rate. σ is the applied stress; A is the power law multiplier, the value is 1.24×10^{-23} , n is the creep exponent, and the value is 7.5.

The mechanical properties of the material is given in Table 1.

Table 1. Material mechanical property of Nickel-based alloy 600 at 343°C

Material	E /MPa	ν	σ_0 /MPa	n	α
Alloy600	193 000	0.288	385	4.799	1.0

2.3. Loading and boundary conditions

Due to symmetry of CT specimen, only the half specimen was modelled. Boundary condition is applied to the symmetry plane of the model in Y direction, and to the load application in the X direction, as shown in Figure 2(a). Loading is applied to the load hole by using the multiple point constraints facility in ABAQUS, which joins the hole centre to the nodes of the hole surface. The concentrated force is applied on the reference point to ensure the crack tip stress intensity factor $K_I=15 \text{ MPa}\cdot\text{m}^{1/2}$.

3. Results and Discussion

3.1. Effect of specimen thickness on SCC crack tip stress

The Mises stress distribution in front of the crack tip of different thickness samples is shown in Figure 3. The radius is 0.5 mm, and it can be seen that the Mises stress decreases with increasing of the specimen thickness. The Mises stress decreases slowly as the thickness increases when thickness ratio ≥ 0.1 , that is to say, The effect of thickness on the Mises stress at this time is not so great.

3.2. Effect of specimen thickness on SCC crack tip PEEQ

The PEEQ distribution in front of the crack tip of different thickness samples is shown in Figure 4. The radius is also set as 0.5 mm. The PEEQ at crack tip decreases with the increasing of the specimen thickness, but the influence is not so obvious, which indicates that PEEQ at crack tip is not a appropriate parameter to describe crack propagation.

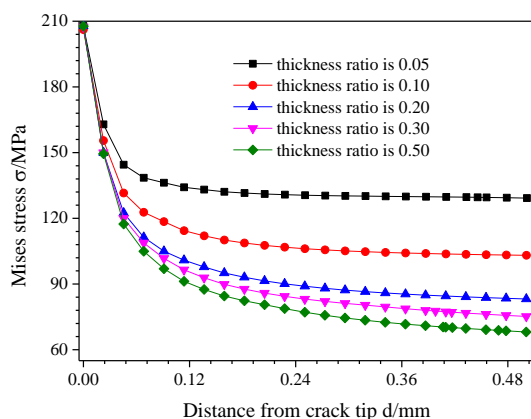


Figure 3. Mises stress ahead of crack tip (MPa)

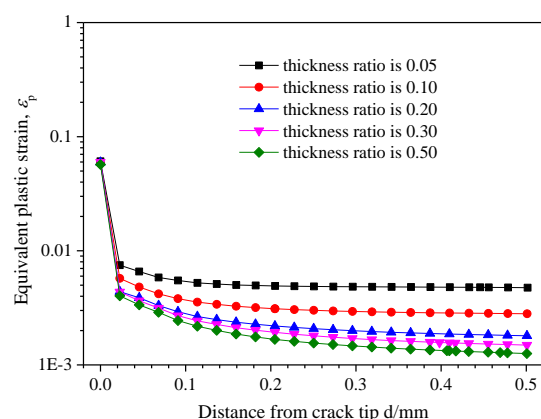


Figure 4. Tensile plastic strain ahead of crack tip

3.3. Effect of specimen thickness on SCC crack tip creep strain

The creep strain distribution in front of the crack tip of different thickness samples is shown in Figure 5. The creep strain at crack tip decreases with the increasing of the specimen thickness, but the influence is not so obvious, which indicates that creep strain at crack tip is not a appropriate parameter to describe crack propagation.

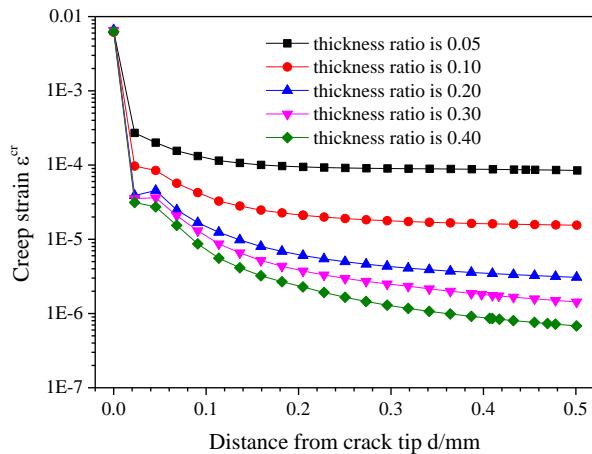


Figure 5. Creep strain ahead of crack tip

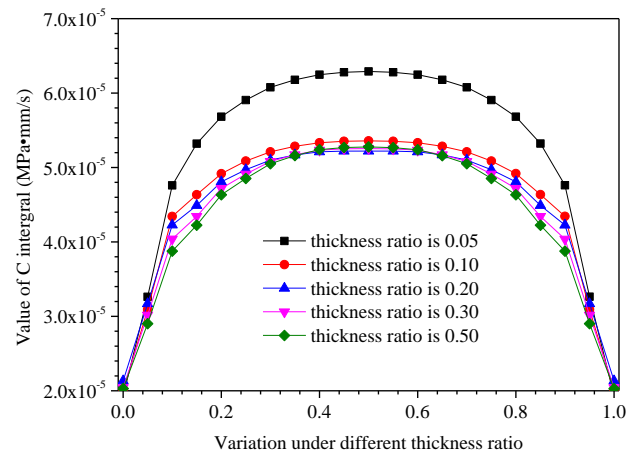


Figure 6. Value of C integral

3.4. Effect of specimen thickness on C integral

The effect of specimen thickness on the crack tip C integration is shown in Figure 6. The value of the C-integral decreases gradually as the thickness of the sample increase, so the constraint is larger when specimen is greater, and the specimen is less likely to crack at this time. Compared with the thinner sample, the crack growth rate is also smaller due to the thicker specimen being closer to the plane stress state. Compared with the stress and strain parameters, C integral is a reasonable crack tip fracture parameter, suitable for describing the crack initiation and growth of stress corrosion cracking.

4. Conclusions

By analyzing the influence of the thickness of the compact tensile specimen on the creep stress-strain field at the crack tip of the Ni-based alloy SCC, the conclusions are as follows:

- (1) When the sample thickness ratio $B/W \geq 0.1$, the crack tip effect is almost ineffective; when $B/W = 0.25$, The crack tip stress, strain and C integral is the maximum, then the specimen thickness has little effect on the C integral value.
- (2) Compared with the stress and strain parameters, C integral is a reasonable crack tip fracture parameter, suitable for describing the crack initiation and expansion of stress corrosion cracking.
- (3) To accurately predict the crack propagation rate of the low-constraint nuclear welding structure, it is necessary to consider the influence of the constraint level of the specimen on the crack propagation rate.

Acknowledgments

This work is financially supported by the National Natural Science Foundation of China (Grant nos. are 51475362 and 11502195).

References

- [1] Ma Cheng, Peng Qunjia, Han Enhou. Review of stress corrosion cracking of structural materials in nuclear power plants [J]. Journal of Chinese Society for Corrosion and Protection, 2014, 34(1): 37-45.
- [2] Xue He, Gong Xiaoyan, Zhao Lingyan. Effect of mechanical parameter selection in Quantitative estimation of the growth of environmentally assisted cracks at flaws in light water

- reactor components with complex mechanical condition[C]. ASME 2011 Pressure Vessels and Piping Conference, 2011: 893-899.
- [3] PENG Qunjia, XUE He, HOU Juan. Role of water chemistry and microstructure in stress corrosion cracking in the fusion boundary region of an Alloy 182-A533B low alloy steel dissimilar weld joint in high temperature water [J]. Corrosion Science, 2011, 53(12): 4309-4317.
- [4] Tan Jianping, WANG Guozhen, XUAN Fuzhen, et al. The effect of CT specimen thickness on high temperature creep crack growth rate of 25Cr2NiMo1V steel [J]. Materials for Mechanical Engineering, 2012, 36(10): 42-46.
- [5] Kim Y J, Kim J S, CHO S M, et al. 3-D constraint effects on J testing and crack tip constraint in M(T), SE(B), SE(T) and C(T) specimens: numerical study [J]. Engineering Fracture Mechanics, 2004, 71(9): 1203-1218.
- [6] Dodds Jr R H, Shih C F, Anderson T L. Continuum and micro mechanics treatment of constraint in fracture [J]. International Journal of Fracture, 1993, 64(2): 101-133.
- [7] Mostafavi M, Smith D J, Pavier M J. A micromechanical fracture criterion accounting for in-plane and out-of-plane constraint [J]. Computational Materials Science, 2011, 50: 2759-2770.
- [8] Yand Jie, Wand Guozhen, Xuan Fuzhen. Unified characterisation of in-plane and out-of-plane constraint based on crack-tip equivalent plastic strain [J]. Fatigue & Fracture of Engineering Materials & Structures, 2013, 36(6): 504-514.
- [9] He Bin, Liu Jun, Chen Jianen, et al. Finite element simulation of the growth rate of high temperature creep crack of P92 steel with different constraints [J]. Materials Review, 2016, 30(16): 145-149.
- [10] ASTM Standard E399-90. Annual book of ASTM standards[M]. USA: ASTM International, 2002.
- [11] Ueda Y, Shi Y, Sun S. Effect of crack depth and strength mis-matching on the relation between J-integral and CTOD for welded tensile specimens(mechanics, strength & structure design) [J]. Transaction of JWRI, 1997, 26(1): 133-140.
- [12] Zhao Lingyan, Cui Yinghao, Xue He, et al. Effect of crack propagation initiation angle on the stress corrosion cracking behavior in welding transition zone of Ni-based alloys [J]. China Sciencepaper, 2016, 11(16): 1864-1866.
- [13] Quintero H, Mehmanparast A. Prediction of creep crack initiation behaviour in 316H stainless steel using stress dependent creep ductility[J]. International Journal of Solids & Structures, 2016, s 97-98:101-115.